

Soliton Defects in One-dimensional Topological Three-band Hamiltonian

Gyungchoon Go,¹ Kyeong Tae Kang,¹ and Jung Hoon Han^{1,2,*}

¹*Department of Physics, Sungkyunkwan University, Suwon 440-746, Korea*

²*Asia Pacific Center for Theoretical Physics, POSTECH, Pohang, Gyeongbuk 790-784, Korea*

Defect formation in the one-dimensional topological three-band model is examined within both lattice and continuum models. Classic results of Jackiw-Rebbi and Rice-Mele for the soliton charge is generalized to the three-band model. The presence of the central flat band in the three-band model makes the soliton charge as a function of energy behave in a qualitatively different way from the two-band Dirac model case. Quantum field-theoretical calculation of Goldstone and Wilczek is also generalized to the three-band model to obtain the soliton charge. Diamond-chain lattice is shown to be an ideal structure to host a topological three-band structure.

PACS numbers: 72.15.Nj, 11.10.Ef

Introduction.- Defects are a useful way of unearthing topological properties of the underlying band structure [1, 2]. A classic example is the Su-Schrieffer-Heeger solitonic defect formed at the kink of a Peierls insulator [1]. Its existence as the mid-gap state is a manifestation of the massive Dirac nature of bulk one-dimensional band. Soliton nucleation due to π -flux threading a two-dimensional topological band insulator is another example of the defect revealing the topological nature of the bulk band [2]. In all known instances so far, however, the physics near the gap-opening momentum is treated within the two-component Dirac theory drawn from the upper and the lower bands (Fig. 1(a)). The well-known Jackiw-Rebbi mechanism [3] then automatically produces a soliton at the mass sign-changing point. Later Jackiw-Rebbi model was generalized to treat cases without the particle-hole symmetry, which gives rise to solitons carrying parameter-dependent irrational charge [4–6]. Generalization to cases involving more than two bands, however, had not been made.

One may as well envision situations where the two bands are “intervened” by a third one passing through the gapped region, forming a three-band anti-crossing as schematically shown in Fig. 1(a). A minimal model, although not the most general one [7], for such situation is the three-band Hamiltonian

$$\mathcal{H}_{\mathbf{k}} = \mathbf{d}_{\mathbf{k}} \cdot \mathbf{S} \quad (1)$$

where $\mathbf{S} = (S^x, S^y, S^z)$ are the three components of a spin-1 matrix and $\mathbf{d}_{\mathbf{k}}$ is some momentum (\mathbf{k})-dependent vector. Its energy spectrum has one flat band, $\varepsilon_{\mathbf{k}} = 0$, in addition to a pair of symmetrically placed bands at $\varepsilon_{\mathbf{k}} = \pm|\mathbf{d}_{\mathbf{k}}|$ [8, 9]. Such lattice model in two dimensions can be realized as complex-valued tight-binding Kagome model at special fluxes [9], or in the CuO_2 plane of the cuprates [8]. Bulk topological properties of two-dimensional lattice models of this sort were examined in the past [8–10]. In this paper, we address the nature of those defects formed at the domain boundary in

one-dimensional topological three-band models.

One-dimensional topological three-band model.- We begin by addressing the question: what kind of one-dimensional lattice Hamiltonians would map onto $\mathcal{H}_{\mathbf{k}} = \mathbf{d}_{\mathbf{k}} \cdot \mathbf{S}$ in momentum (k) space? After experimenting with various possible structures we arrive at the so-called diamond-chain lattice [13] as the most likely candidate supporting such bands. Two routes can be followed to construct the model. One is by generalizing the Rice-Mele two-band model [4]. Schematics of such a lattice is depicted in Fig. 1(b). Hopping amplitudes along the sides are modulated as $t + \delta t$ (two lines) and $t - \delta t$ (one line). On-site energies at the two opposing sites, labeled a and b in Fig. 1(b), are introduced as $\pm m$. There are four degenerate ground state configurations - two of which are shown in Fig. 1(b) - in such a model. Choosing the vacuum configuration shown on the left of Fig. 1(b), for instance, yields the k -space Hamiltonian

$$\begin{aligned} H^I &= \sum_k \Psi_k^\dagger \left[2 \left(\sqrt{2} t \cos k, \sqrt{2} \delta t \sin k, m \right) \cdot \mathbf{S} \right] \Psi_k \\ &\equiv \sum_k \Psi_k^\dagger \mathcal{H}_k^I \Psi_k, \end{aligned} \quad (2)$$

where $\Psi_k^T = (\psi_k^a, \psi_k^c, \psi_k^b)$. Definition of the Fourier modes are $a_{2n} = \frac{1}{\sqrt{N}} \sum_k e^{-2ikn} a_k$ (similarly b_{2n+1} and c_{2n}), where N is number of a -sites (equivalently, b or c -sites). Representation of the spin matrix \mathbf{S} is such that S^z is diagonal, with entries $+1, 0, -1$.

A second class of topological three-band Hamiltonians is found by considering flux models. Introducing the diagonal hopping between a and c sites creates triangles that may be threaded with internal flux, despite the overall lattice being one-dimensional. Choosing the real-space hopping patterns as shown in Fig. 1(c) results in the Hamiltonian

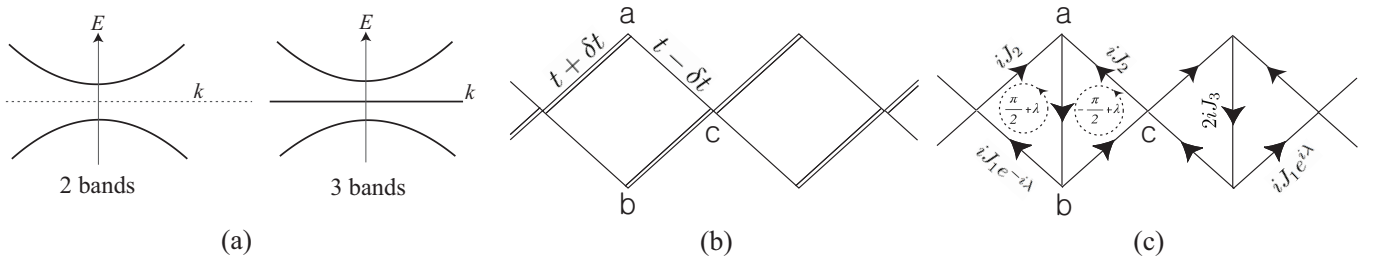


FIG. 1: (a) Schematic picture of the generic two-band (left) vs. three-band (right) anti-crossing in a band structure. (b) The ground state hopping configuration in the diamond-chain lattice model of H^I . (c) Hopping patterns for H^{II} . Flux penetrating the two triangles are $\pm\pi/2 + \lambda$, respectively.

$$\begin{aligned}
 H^{II} &= \sum_k \Psi_k^\dagger \left[2 \left(J_1 \cos(k+\lambda), J_2 \cos k, J_3 \right) \cdot \mathbf{S} \right] \Psi_k \\
 &\equiv \sum_k \Psi_k^\dagger \mathcal{H}_k^{II} \Psi_k.
 \end{aligned} \quad (3)$$

This time, $\Psi_k^T = (\psi_k^a, \psi_k^b, \psi_k^c)$ and the spin matrices are given by $(S^\alpha)_{\beta\gamma} = -i\varepsilon_{\alpha\beta\gamma}$. Flux penetrating the two triangles are $\pm\pi/2 + \lambda$, respectively [11].

Both constructions lead to the structure $\mathcal{H}_k = \mathbf{d}_k \cdot \mathbf{S}$, in different representations of the spin matrices. Mathematically they may be related by a unitary transformation, but physically H^I and H^{II} represent quite different situations (modulated real-valued hopping vs. complex-valued hopping, on-site energy difference vs. diagonal hopping, etc.). It is encouraging that very different physical conditions can result in the same general Hamiltonian. In both models the first Brillouin zone extends over $-\pi/2 < k \leq \pi/2$, although the periodicity of the Hamiltonian is 2π : $\mathcal{H}_{k+2\pi}^{I,II} = \mathcal{H}_k^{I,II}$. A related observation was made for two-dimensional topological three-band models earlier [8, 9], and readers may consult them regarding this point.

Topological quantum numbers associated with the band Hamiltonians H^I and H^{II} can be readily computed in terms of a two-component unit vector $\hat{\mathbf{n}}^a(k) = \mathbf{n}^a(k)/|\mathbf{n}^a(k)| \equiv (\cos\theta_k^a, \sin\theta_k^a)$, as the integral $N^a = (1/2\pi) \int_{-\pi}^{\pi} (d\theta_k^a/dk)$ [12]:

$$\begin{aligned}
 \mathbf{n}^I(k) &= (t \cos k, \delta t \sin k), \quad N^I = \text{sgn}(t\delta t), \\
 \mathbf{n}^{II}(k) &= (J_1 \cos(k+\lambda), J_2 \cos k), \quad N^{II} = \text{sgn}(\lambda J_1 J_2).
 \end{aligned} \quad (4)$$

Boundary states.- In a physical system with nontrivial topological index there may exist localized states near boundaries. In both models with open boundaries as shown in Fig. 2(a) and (b), there are pairs of localized defect states, one per boundary, at energies

$$E_s^I = \pm 2m, \quad E_s^{II} = \pm 2J_3, \quad (5)$$

with the localization factors $(\psi_{2j}^{a,b,c} = \rho^j \psi_0^{a,b,c})$

$$\rho^I = -\frac{t^2 - \delta t^2}{(t \pm \delta t)^2}, \quad \rho^{II} = -\frac{J_1^2 e^{2i\lambda} + J_2^2}{J_1^2 + J_2^2 \mp 2J_1 J_2 \sin \lambda}. \quad (6)$$

The \pm sign in Eq. (6) gives either the left- or the right-localized mode depending on signs of $t\delta t$, $J_1 J_2$ and λ [14]. Having found some localized states, the next obvious questions are whether these localized states represent the generalization of the familiar Su-Schrieffer-Heeger soliton state [1] to the three-band model, and, if so, what is the associated charge of the soliton? These are issues that cannot be answered within the tight-binding analysis alone. For this we turn to the continuum theory as pioneered by the field theorists [3, 6, 15] and show how they can be generalized to solitons arising in the three-band model.

Continuum theory of the three-band soliton.- In contrast to the two-band Su-Schrieffer-Heeger soliton state that has received enormous scrutiny in terms of continuum theory, there appears little, if at all, attempt in the literature to construct a field-theoretical continuum description of the three-band defect such as found here. We aim at establishing such continuum theory now and use it to compute the charge of the soliton. Only one of the Hamiltonians H^I and H^{II} needs to be analyzed for this purpose as the calculated soliton charge will be invariant under the unitary transformation. We choose H^I , rescale $t \rightarrow t/\sqrt{2}$ and $\delta t \rightarrow \delta t/\sqrt{2}$, and expand it around $k = \pi/2$ where one obtains both the maximum topological density $|d\theta_k^I/dk|$ and the minimum gap. Choosing $t = 1$, one finds the real-space Hamiltonian

$$\mathcal{H} = 2 \left[(i\partial_x) S^x + \delta t S^y + m S^z \right], \quad (7)$$

where the superscript I has been dropped. Particle-hole symmetry is generally absent in \mathcal{H} with both δt and m finite [4]. Soliton state occurs thus at non-zero energies, either above the flat band or below, depending on the sign of the kink.

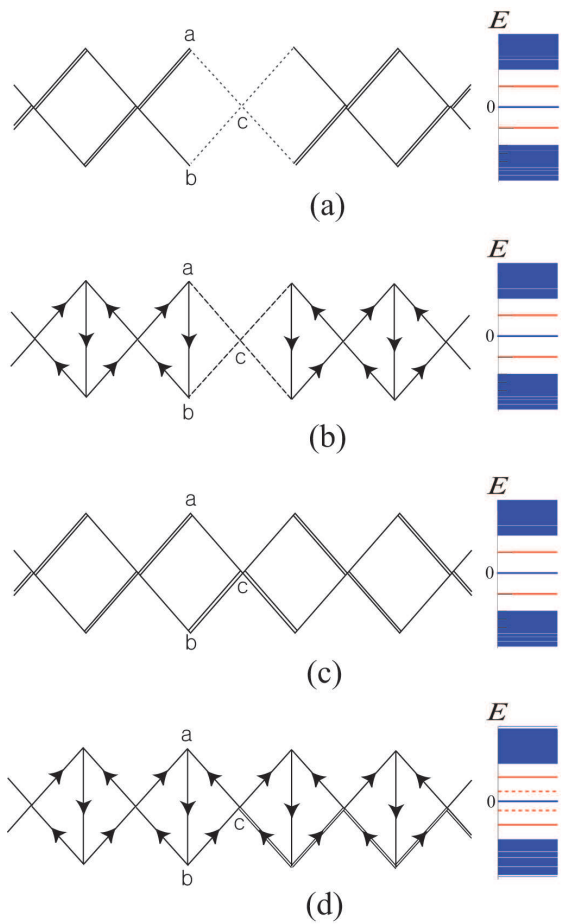


FIG. 2: (color online) Imposing open boundary condition on the models (a) H^I and (b) H^{II} . Hopping amplitudes along the dotted lines are zero. A pair of soliton states are induced on either side of the boundary at energies indicated by red lines in the schematic energy diagram on the right. The center blue line is the flat band at zero energy. (c) Reversing the sign of δt in H^I on half of the lattice sites in a closed chain. One soliton state per sign-reversed site is induced at red-lined energies. (d) Reversing the sign of J_1 on half the lattice sites in H^{II} . Red-dashed energies are split off from the central flat band by perturbative effects and do not represent soliton states of our interest.

In the case where $\delta t(x)$ behaves as a solitonic background, $\delta t(x) = \delta t_0 \text{sgn}(x)$, $m(x) = m_0$, (un-normalized) continuum wave function of the localized state is found [14]

$$\psi(x) \sim \begin{pmatrix} e^{-\delta t_0|x|} \\ 0 \\ 0 \end{pmatrix}, \quad E_s = 2m_0 \quad (\delta t_0 > 0),$$

$$\psi(x) \sim \begin{pmatrix} 0 \\ 0 \\ e^{\delta t_0|x|} \end{pmatrix}, \quad E_s = -2m_0 \quad (\delta t_0 < 0). \quad (8)$$

The above solution, derived for the sign-changing $\delta t(x)$ corresponding to Fig. 2(c), remains also a solution for the

case in Fig. 2(a) because identical boundary conditions ($\psi_{2j}^b = 0$) are met by the lattice soliton solutions in both (a) and (c).

We were able to adapt the method of Ref. [6] to calculate the soliton charge of the state found in Eq. (9) [14]. The amount of fractional state lost from the valence band to the soliton, ΔN_v , equals

$$\Delta N_v = \frac{2}{\pi} \tan^{-1} \left(\left| \frac{\delta t_0}{m_0} \right| \right), \quad E_s = 2|m_0|, \quad (m_0 \delta t_0 > 0),$$

$$\Delta N_v = \frac{2}{\pi} \tan^{-1} \left(\left| \frac{m_0}{\delta t_0} \right| \right), \quad E_s = -2|m_0|, \quad (m_0 \delta t_0 < 0). \quad (9)$$

The loss from the conduction band ΔN_c is one minus this number, and together contributes $\Delta N_v + \Delta N_c = 1$ toward the formation of one soliton defect while the flat band does not give up any state to it. Soliton charge Q_s is minus the fractional loss from the valence band: $Q_s = -\Delta N_v$. A corresponding two-band model, obtained by replacing $S = 1$ spin operator \mathbf{S} by the Pauli matrix $\boldsymbol{\sigma}$ in Eq. (7), yields $\Delta N_v = 1/2 - (1/\pi) \tan^{-1}(m_0/\delta t_0)$ [6]. The two calculated soliton charges, for two- and three-band topological models, are summarized pictorially in Fig. 3.

The amount of soliton charge abruptly changes from 0 to 1 at $m_0 = 0$ even though the soliton energy E_s changes continuously through zero. This stands in sharp contrast to the two-band soliton whose fractional charge smoothly varies through 1/2 at the particle-hole symmetric point $m_0 = 0$. Such discontinuous change of the soliton charge is a distinct feature of the three-band topological model, and sets it apart from the well-known two-band case. The presence of the central flat band, as required by the three-band rather than the two-band character of the model, plays a critical role in the determination of the soliton charge although by itself it does not contribute any states to its formation. For this reason, we believe the reduction of the three-band Hamiltonian $\mathbf{d}_k \cdot \mathbf{S}$ to its two-band counterpart $\mathbf{d}_k \cdot \boldsymbol{\sigma}$, by somehow integrating out the flat band, is unlikely.

Quantum field theory calculation of soliton charge. Computation of the soliton charge above was carried out using the knowledge of quantum-mechanical wave functions in the soliton background. Generalization of the classic Jackiw-Rebbi result to the three-band soliton is thus made feasible. On the other hand Goldstone and Wilczek (GW) [15] showed how to compute the induced soliton charge using the quantum field theory technique. In the following we show that GW's approach, like the wave function method, can be generalized to three-band models.

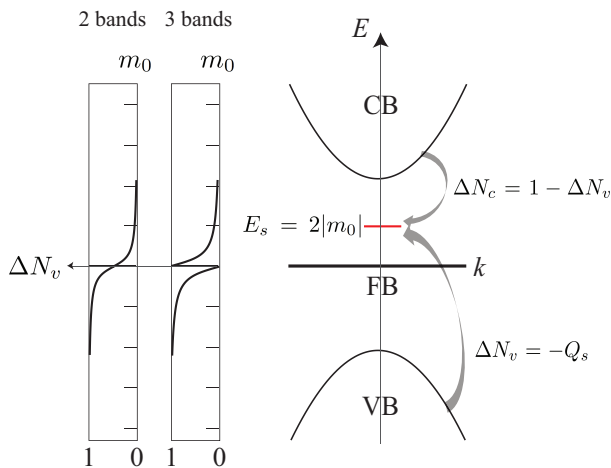


FIG. 3: (color online) Fractional state lost from the valence band ΔN_v for two- and three-band models as a function of the soliton energy on the vertical axis. A schematic picture on the right shows how the conduction band (CB) and the valence band (VB) contribute fractional states ΔN_c and ΔN_v adding up to one soliton state, $\Delta N_c + \Delta N_v = 1$. Flat band (FB) does not lose its states to the soliton.

One begins by writing down a one-dimensional Lagrangian

$$L = \int dx \psi^\dagger (i\partial_t - iS^x \partial_x - \phi_1 S^z - \phi_2 S^y) \psi, \quad (10)$$

where, as in GW's formulation, (ϕ_1, ϕ_2) undergo a rotation by angle $\theta(x)$: $(\phi_1(x), \phi_2(x)) = M(\cos \theta(x), \sin \theta(x))$. Current operator for the fermion field ψ can be written down, $j^\mu = \psi^\dagger \Gamma^\mu \psi$, with a pseudo- Γ matrix $\Gamma^0 = \mathbb{I}$, $\Gamma^1 = S^x$. Calculating the average current using the standard technique [14] yields

$$\langle j^\mu \rangle = -\frac{1}{\pi} \epsilon^{\mu\nu} \partial_\nu \left[\tan^{-1} \left(\frac{\phi_2}{\phi_1} \right) \right], \quad (11)$$

which is *twice* the GW result. In the case where $\phi_2(x)$ behaves as a solitonic background, i.e. $\phi_2(x) \rightarrow \pm \delta t_0$ as $x \rightarrow \pm \infty$ while $\phi_1(x) = m_0$ stays constant, we obtain

$$Q_s = -\frac{2}{\pi} \tan^{-1} \left(\frac{\delta t_0}{m_0} \right). \quad (12)$$

from integrating $\langle j^0 \rangle$ over x . The result agrees with our previous quantum-mechanical calculation of the soliton charge in Eq. (9). Basically this is twice the charge obtained for the two-band Dirac model and as a result the charge approaches unity (rather than half as in the Dirac model) at the particle-hole symmetric point $m_0 = 0$. Since it is the fractional part of the soliton charge which matters, the soliton charge has to drop discontinuously to zero as m_0 passes through zero, as

shown in Fig. 3.

Discussion.- Defects in topological three-band Hamiltonian $H_k = \mathbf{d}_k \cdot \mathbf{S}$ in one dimension were examined with emphasis on developing a three-band analogue to the well-known Jackiw-Rebbi-Su-Schrieffer-Heeger soliton physics in one-dimensional Dirac bands. All the classic results of Jackiw-Rebbi and Goldstone-Wilczek are generalized to the three-band model. We suggest that soliton states carrying irrational quantum numbers may well exist in compounds that embody the crystal structure of the diamond-chain lattice. As a possible candidate material we point out that the α -form of Palladium dichloride (PdCl_2) possesses the diamond-chain structure resembling our model [16]. Analysis carried out in this paper are restricted to a special kind in possession of the central flat band. Re-locating the flat band, say, to be the top band requires going through a quantum phase transition that will also qualitatively change the character of the model, let alone the nature of solitons. It is likely the three-band model whose flat band is located between the valence and the conduction band represents a qualitatively different physical situation from the one where it is located at the top or the bottom of the band structure. The latter case may be reducible to the two-band model plus a trivial flat band, while the former, as we showed through calculation of the soliton charge, represents a new class of models.

We acknowledge fruitful discussions with Alex Altland, Leon Balents, Akira Furusaki, and Hosho Katsura. J. H. H. is supported by the NRF grant (No. 2013R1A2A1A01006430).

* Electronic address: hanjh@skku.edu

- [1] W. P. Su, J. R. Schrieffer, and A. J. Heeger, Phys. Rev. Lett. **42**, 1698 (1979); Phys. Rev. B **22**, 2099 (1980).
- [2] Dung-Hai Lee, Guang-Ming Zhang, and Tao Xiang, Phys. Rev. Lett. **99**, 196805 (2007).
- [3] R. Jackiw and C. Rebbi, Phys. Rev. D **13**, 3398 (1976).
- [4] M. Rice and E. Mele, Phys. Rev. Lett. **49**, 1455 (1982).
- [5] S. Kivelson, Phys. Rev. B **28**, 2653 (1983).
- [6] R. Jackiw and G. W. Semenoff, Phys. Rev. Lett. **50**, 439 (1983); R. MacKenzie and Frank Wilczek, Phys. Rev. D **30**, 2194 (1984).
- [7] The most general three-band Hamiltonian contains eight parameters, one for each Gell-Mann matrix. Analysis of the topological properties in this general case is currently in progress.
- [8] Yan He, Joel Moore, and C. M. Varma, Phys. Rev. B **85**, 155106 (2012).
- [9] Gyungchoon Go, Jin-Hong Park, and Jung Hoon Han, Phys. Rev. B **87**, 155112 (2013).
- [10] Kenya Ohgushi, Shuichi Murakami, and Naoto Nagaosa, Phys. Rev. B **62**, 6065 (2000).
- [11] Relations such as $\mathcal{H}_{-\lambda}^{\text{II}}(k) = \mathcal{H}_{\lambda}^{\text{II}}(-k)$ and $\mathcal{H}_{\lambda+\pi}^{\text{II}}(k) = U^\dagger \mathcal{H}_{\lambda}^{\text{II}}(k) U$ with some unitary matrix U restrict the range

of independent λ values to $0 \leq \lambda \leq \pi/2$.

- [12] Ning Wu, Phys. Lett. A **376**, 3530 (2012).
- [13] Zsolt Gulácsi, Arno Kampf, and Dieter Vollhardt, Phys. Rev. Lett. **99**, 026404 (2007).
- [14] See Supplemental Information for details of the calculation.
- [15] J. Goldstone and F. Wilczek, Phys. Rev. Lett. **47**, 986 (1981).
- [16] Jürgen Evers, Wolfgang Beck, Michael Göbel, Stefanie Jakob, Peter Mayer, Gilbert Oehlinger, Marianne Rotter, and Thomas M. Klapötke, Ang. Chem. **49**, 5677 (2010).

Soliton Defects in One-dimensional Topological Three-band Hamiltonian: Supplemental Information

Gyungchoon Go,¹ Kyeong Tae Kang,¹ and Jung Hoon Han^{1,2}

¹*Department of Physics, Sungkyunkwan University, Suwon 440-746, Korea*

²*Asia Pacific Center for Theoretical Physics, POSTECH, Pohang, Gyeongbuk 790-784, Korea*

I. LATTICE CALCULATION OF THE BOUNDARY STATE

In this section we discuss how to obtain the localized solutions at the open boundaries of the two models,

$$\begin{aligned} H^I &= \sum_k \Psi_k^\dagger \left[2 \left(\sqrt{2} t \cos k, \sqrt{2} \delta t \sin k, m \right) \cdot \mathbf{S} \right] \Psi_k, \\ H^{II} &= \sum_k \Psi_k^\dagger \left[2 \left(J_1 \cos(k+\lambda), J_2 \cos k, J_3 \right) \cdot \mathbf{S} \right] \Psi_k. \end{aligned} \quad (1.1)$$

In real space the first Hamiltonian becomes

$$\begin{aligned} H^I &= \sum_{n=0}^N \left[m \left(a_{2n}^\dagger a_{2n} - c_{2i}^\dagger c_{2n} \right) \right. \\ &\quad + (t - \delta t) \left(a_{2n}^\dagger b_{2n+1} + b_{2n+1}^\dagger c_{2n+2} + h.c. \right) \\ &\quad \left. + (t + \delta t) \left(b_{2n+1}^\dagger c_{2n} + b_{2n+1}^\dagger a_{2n+2} + h.c. \right) \right]. \end{aligned} \quad (1.2)$$

Using the one-particle wave function

$$|\Psi\rangle = \sum_j \left(\psi_{2j}^a a_{2j}^\dagger + \psi_{2j+1}^b b_{2j+1}^\dagger + \psi_{2j}^c c_{2j}^\dagger \right) |0\rangle, \quad (1.3)$$

and the Schrödinger equation $H^I|\Psi\rangle = E^I|\Psi\rangle$ we obtain the equations

$$\begin{aligned} E^I \psi_{2j}^a &= m \psi_{2j}^a + (t - \delta t) \psi_{2j+1}^b + (t + \delta t) \psi_{2j-1}^b, \\ E^I \psi_{2j+1}^b &= (t - \delta t) \psi_{2j}^a + (t + \delta t) \psi_{2j+2}^a \\ &\quad + (t - \delta t) \psi_{2j+2}^c + (t + \delta t) \psi_{2j}^c, \\ E^I \psi_{2j}^c &= -m \psi_{2j}^c + (t - \delta t) \psi_{2j-1}^b + (t + \delta t) \psi_{2j+1}^b. \end{aligned} \quad (1.4)$$

In order to obtain the boundary states we choose the open boundary conditions

$$\psi_1^b = \psi_{2N-1}^b = 0, \quad (1.5)$$

and insert it into (1.4). There are four equations satisfied at the boundaries:

$$\begin{aligned} E^I \psi_2^a &= m \psi_2^a + (t - \delta t) \psi_3^b, \\ E^I \psi_2^c &= -m \psi_2^c + (t + \delta t) \psi_3^b, \\ E^I \psi_{2N-2}^a &= m \psi_{2N-2}^a + (t + \delta t) \psi_{2N-3}^b, \\ E^I \psi_{2N-2}^c &= -m \psi_{2N-2}^c + (t - \delta t) \psi_{2N-3}^b. \end{aligned} \quad (1.6)$$

For the exponentially localized solution we assume the following ansatz

$$\psi_{2j+2}^{a,c} = \rho^j \psi_2^{a,b}, \quad \psi_{2j+3}^b = \rho^j \psi_3^b. \quad (1.7)$$

Using (1.4), (1.6), and (1.7) we obtain

$$\begin{aligned} E^I = 2m, \quad \rho^I &= -\frac{t^2 - \delta t^2}{(t + \delta t)^2}, \quad \psi_{2j}^b = \psi_{2j+1}^c = 0, \\ E^I = -2m, \quad \rho^I &= -\frac{t^2 - \delta t^2}{(t - \delta t)^2}, \quad \psi_{2j}^a = \psi_{2j+1}^c = 0. \end{aligned} \quad (1.8)$$

If one solution is left-localized ($|\rho| < 1$) the other one ($|\rho| > 1$) must be localized at the right boundary. By the same manipulation one can easily derive the boundary state of the second model H^{II}

$$E^{II} = \pm 2J_3, \quad \rho^{II} = -\frac{J_1^2 e^{2i\lambda} + J_2^2}{J_1^2 + J_2^2 \mp 2J_1 J_2 \sin \lambda}, \quad \psi_{2j+1}^c = 0. \quad (1.9)$$

II. CONTINUUM SOLITON SOLUTION

Here we work out the soliton solution of the continuum Hamiltonian

$$\begin{aligned} \mathcal{H}^I &= 2(S^x i \partial_x + \delta t(x) S^y + m(x) S^z) \\ &= 2 \begin{pmatrix} m & \frac{-i}{\sqrt{2}}(\delta t(x) - \partial_x) & 0 \\ \frac{i}{\sqrt{2}}(\delta t(x) + \partial_x) & 0 & \frac{-i}{\sqrt{2}}(\delta t(x) - \partial_x) \\ 0 & \frac{i}{\sqrt{2}}(\delta t(x) + \partial_x) & -m \end{pmatrix}, \end{aligned} \quad (2.1)$$

with the background domain-wall profile, $\delta t(x) = \text{sgn}(x) \delta t_0$ and $m(x) = m_0$. Solving the Schrödinger equation, $\mathcal{H}^I \psi(x) = E \psi(x)$, where $\psi^T(x) = (u(x), v(x), w(x))$, we have the three equations

$$\begin{aligned}\frac{-i}{\sqrt{2}}(\delta t(x) - \partial_x)v &= (E - m)u \\ \frac{i}{\sqrt{2}}(\delta t(x) + \partial_x)v &= (E + m)w, \\ \frac{i}{\sqrt{2}}(\delta t(x) + \partial_x)u - \frac{i}{\sqrt{2}}(\delta t(x) - \partial_x)w &= Ev. \end{aligned} \quad (2.2)$$

For the exponentially localized solution we take

$$u(x) = u_0 e^{-\kappa|x|}, v(x) = v_0 e^{-\kappa|x|}, w(x) = w_0 e^{-\kappa|x|}. \quad (2.3)$$

Inserting (2.3) into (2.2) we obtain a pair of solutions,

$$\begin{aligned} E = m, \quad \delta t_0 = \kappa, \quad w_0 = v_0 = 0, \\ \text{or } E = -m, \quad \delta t_0 = -\kappa, \quad u_0 = v_0 = 0. \end{aligned} \quad (2.4)$$

III. CALCULATION OF THE SOLITON CHARGE

Calculating the amount of states missing from the scattering states, which instead contributed to the formation of a soliton bound state, is a tricky issue. We found it advisable to build up both intuition and the necessary technology for the charge calculation with a familiar example of one-dimensional Schrödinger equation, adapted later to the problem of soliton charge in the three-band case.

Take the Schrödinger problem

$$[-\partial_x^2 + 2\kappa\delta(x)]u(x) = \varepsilon u(x) \quad (3.1)$$

allowing for either signs of the delta-potential, $\kappa > 0$ or $\kappa < 0$. The scattering states are constructed as

$$\begin{aligned} u_L(x) &= e^{ikx} + R_k e^{-ikx} \\ u_R(x) &= T_k e^{ikx} \end{aligned} \quad (3.2)$$

where L/R refer to the left/right of the delta-potential. Matching the boundary conditions readily yields

$$T_k = \frac{ik}{ik - \kappa}, \quad R_k = \frac{\kappa}{ik - \kappa} \quad (3.3)$$

The normalization of the wave function is such that $\int_{-L/2}^{L/2} |u(x)|^2 dx = L$, instead of 1. We ignore small corrections of order $O(1/L)$ in the evaluation of the normalization factor. The scattering states in the presence of the delta-potential will be denoted $u^{(\delta)}(x)$, and those in its absence, $u^{(0)}(x)$. Naively, one might think the number of missing scattering states is obtained by the integral

$$\Delta Q \equiv \int_{-\infty}^{\infty} \frac{dk}{2\pi} \int_{-L/2}^{L/2} dx \left(|u_k^{(\delta)}(x)|^2 - |u_k^{(0)}(x)|^2 \right). \quad (3.4)$$

Direct insertion of the wave functions obtained earlier with the x integral $\int_0^\infty dx e^{ikx} = i/k + \pi\delta(k)$ leads to the formula

$$\Delta Q = - \int_{-\infty}^{\infty} \frac{dk}{2\pi} \frac{\text{Im}[R_k]}{k} - \frac{1}{2} = \frac{\text{sgn}(\kappa)}{2} - \frac{1}{2}. \quad (3.5)$$

It is obvious that $\Delta Q = -1$ for the attractive case ($\kappa < 0$) and $\Delta Q = 0$ for the repulsive one ($\kappa > 0$). It simply counts whether a bound state has been formed by the potential or not, and it is only the attractive case that will generate one exponentially bound state.

Backed by this exercise, we will study how the state counting goes for the three-band problem. The eigenvalue problem one needs to solve is

$$\begin{aligned} m u_{k,\varepsilon_k} - \frac{i}{\sqrt{2}}(\delta t - \partial_x)v_{k,\varepsilon_k} &= \varepsilon_k u_{k,\varepsilon_k}, \\ \frac{i}{\sqrt{2}}(\delta t + \partial_x)u_{k,\varepsilon_k} - \frac{i}{\sqrt{2}}(\delta t - \partial_x)w_{k,\varepsilon_k} &= \varepsilon_k v_{k,\varepsilon_k} \\ \frac{i}{\sqrt{2}}(\delta t + \partial_x)v_{k,\varepsilon_k} - m w_{k,\varepsilon_k} &= \varepsilon_k w_{k,\varepsilon_k} \end{aligned} \quad (3.6)$$

at momentum k and energy $E_k = 2\varepsilon_k$. There may be a bound-state solution in addition to the scattering solutions characterized by the wave number k . Soliton profile is generally offered by the functional form $\delta t(x) = \delta t_0 \tanh(\xi x)$, with $\delta t(x)$ varying from $-\delta t_0$ to $+\delta t_0$ between $x = -\infty$ and $x = +\infty$. Unfortunately we were not able to find exact scattering solutions for finite ξ . Instead we will consider $\xi \rightarrow \infty$ where $\delta t(x) = \delta t_0 \text{sgn}(x)$, $\delta t^2(x) = \delta t_0^2$, and $\partial_x \delta t(x) = 2\delta t_0 \delta(x)$. This limit is sufficiently weak so that it gives only one bound state. Solving the Schrödinger equation with the soliton background we obtain

$$\psi_k(x) = \sqrt{\frac{\varepsilon_k^2 - m_0^2}{2\varepsilon_k^2}} \begin{pmatrix} -\frac{i}{\sqrt{2}(\varepsilon_k - m_0)}(\delta t - \partial_x)v_k \\ v_k \\ \frac{i}{\sqrt{2}(\varepsilon_k + m_0)}(\delta t + \partial_x)v_k \end{pmatrix}, \quad (3.7)$$

where $\varepsilon_k = -\sqrt{k^2 + \delta t_0^2 + m_0^2}$ and v_k is the properly normalized negative-energy solution satisfying

$$\left(-\partial_x^2 + \frac{2m_0\delta t_0}{\varepsilon_k} \delta(x) \right) v_k = (\varepsilon_k^2 - m_0^2 - \delta t_0^2) v_k, \quad (3.8)$$

and $\int_{-L/2}^{L/2} |v_k(x)|^2 dx = \int_{-L/2}^{L/2} \psi_k^\dagger(x) \psi_k(x) dx = L$. The normalization chosen above is correct up to corrections

of order $O(1/L)$ which of course should vanish in the large- L limit.

For each value of k , Eq. (3.8) is equivalent to the single-particle Schrödinger equation subject to the δ -function potential, thus the existence of the bound state is determined by the sign of the potential. Since at the moment we are interested in the negative-energy states, ε_k is negative and v_k^s would have no bound state for $m_0\delta t_0 < 0$. Instead, in the case where $m_0\delta t_0 > 0$ one

expect one bound state in v_k^s . Henceforth we will assume $m_0\delta t_0 > 0$.

Integrating the charge density difference

$$\rho_k^s(x) - \rho_k^0(x) = \psi_k^{s\dagger}(x)\psi_k^s(x) - \psi_k^{0\dagger}(x)\psi_k^0(x), \quad (3.9)$$

over all space x and momenta k yields the soliton charge (the superscript s denotes the soliton system and 0, the soliton-free system)¹.

$$\begin{aligned} \Delta Q &= \int_{-L/2}^{L/2} dx \int_{-\infty}^{\infty} \frac{dk}{2\pi} [\rho_k^s(x) - \rho_k^0(x)] = \int dx \int \frac{dk}{2\pi} \left\{ (|v_k^s|^2 - |v_k^0|^2) \right. \\ &\quad \left. + \frac{\varepsilon_k^2 + m_0^2}{4\varepsilon_k^2(\varepsilon_k^2 - m_0^2)} \partial_x^2 (|v_k^s|^2) + \frac{m_0}{\varepsilon_k(\varepsilon_k^2 - m_0^2)} \partial_x (\delta t(x) |v_k^s|^2) - \frac{m_0\delta t_0}{2\varepsilon_k^3} |v_k^s|^2 \delta(x) \right\}. \end{aligned} \quad (3.10)$$

In order to compute the charge difference ΔQ , we solve the Schrödinger equation (3.8). The solution is given as

$$v_k^s(x < 0) = e^{ikx} + R_k e^{-ikx}, \quad v_k^s(x > 0) = T_k e^{ikx}, \quad (3.11)$$

where

$$T_k = \frac{ik\varepsilon_k}{ik\varepsilon_k - \delta t_0 m_0}, \quad R_k = T_k - 1 = \frac{\delta t_0 m_0}{ik\varepsilon_k - \delta t_0 m_0}. \quad (3.12)$$

The expression of the coefficients remains valid for both signs of the energy ε_k . For the valence band, one can use the dispersion $\varepsilon_k = -\sqrt{k^2 + \delta t_0^2 + m_0^2}$ to complete the evaluation of the charge

$$\begin{aligned} \Delta Q_v &= \int dx \int \frac{dk}{2\pi} (|v_k^s|^2 - |v_k^0|^2) + \int \frac{dk}{2\pi} \left[\frac{\delta t_0 m_0}{\sqrt{k^2 + \delta t_0^2 + m_0^2}(k^2 + m_0^2)} (|T_k|^2 + |R_k|^2 + 1) - \frac{\delta t_0 m_0}{(k^2 + \delta t_0^2 + m_0^2)^{\frac{3}{2}}} |T_k|^2 \right] \\ &= -\frac{1}{2} - \int \frac{dk}{2\pi} \frac{1}{k} \text{Im}(R_k) + \frac{2}{\pi} \tan^{-1} \frac{m_0}{\delta t_0} - \int \frac{dk}{2\pi} \left[\frac{\delta t_0 m_0}{\sqrt{k^2 + \delta t_0^2 + m_0^2}} \frac{k^2}{(k^2 + \delta t_0^2)(k^2 + m_0^2)} \right] \\ &= -\frac{1}{2} + \frac{2}{\pi} \tan^{-1} \frac{m_0}{\delta t_0} + \left[\frac{1}{\pi} \tan^{-1} \frac{\delta t_0}{m_0} + \frac{1}{\pi} \tan^{-1} \frac{m_0}{\delta t_0} \right] \\ &= -1 + \frac{2}{\pi} \tan^{-1} \frac{m_0}{\delta t_0} = -\frac{2}{\pi} \tan^{-1} \left| \frac{\delta t_0}{m_0} \right|. \end{aligned} \quad (3.13)$$

Here we used $|T_k|^2 + |R_k|^2 = 1$ and $\int_0^\infty dx e^{ikx} = i/k + \pi\delta(k)$.

For the conduction band, on the other hand, similar manipulation with the positive dispersion $\varepsilon_k = \sqrt{k^2 + \delta t_0^2 + m_0^2}$ yields

$$\Delta Q_c = -\frac{2}{\pi} \tan^{-1} \left| \frac{m_0}{\delta t_0} \right|. \quad (3.14)$$

From Eqs. (3.13) and (3.14) we obtain $\Delta Q_v + \Delta Q_c = -1$. The vacancy of one state from the continuum bands is responsible for the occurrence of one mid-gap bound state at energy $E_s = 2|m_0|$. The argument, and the derivation, remains unchanged whether one takes $\delta t_0 > 0$ and $m_0 > 0$, or the opposite, $\delta t_0 < 0$ and $m_0 < 0$. In both cases the bound state energy is on the positive side $E_s = 2|m_0|$. The soliton charge (more precisely the loss of fractional states) contributed by each band is given by

the same formulas, Eqs. (3.13) and (3.14).

IV. QUANTUM FIELD THEORY CALCULATION OF SOLITON CHARGE

Here we compute the soliton charge of the model by using quantum field theory. From the continuum Hamiltonian, we easily derive the Lagrangian

$$L = \int dx \psi^\dagger(x) (i\partial_t - iS^x \partial_x - \phi_1(x)S^z - \phi_2(x)S^y) \psi(x), \quad (4.1)$$

here we replaced $\delta t(x)$ and $m(x)$ to $\phi_2(x)$ and $\phi_1(x)$. Then we take the unitary transformation

$$\psi \rightarrow U\psi, \quad \psi^\dagger \rightarrow \psi^\dagger U^\dagger, \quad (4.2)$$

which transforms

$$\phi_1 S^z + \phi_2 S^y \longrightarrow \sqrt{\phi_1^2 + \phi_2^2} S^z \equiv M S^z, \quad (M \geq 0). \quad (4.3)$$

We assume M is much larger than the gradients of $\phi_{1,2}^2$. The desired rotation is accomplished by writing $(\phi_1, \phi_2) = M(\cos \theta, \sin \theta)$,

$$U = \exp(i\theta S^x), \quad \theta = \tan^{-1}(\phi_2/\phi_1). \quad (4.4)$$

The Lagrangian after the unitary rotation reads

$$\begin{aligned} L \rightarrow L' &= \int dx \psi^\dagger(x) (i\partial_t + a_t - iS^x \partial_x - S^x a_x - M S^z) \psi(x) \\ &= \int dx \psi^\dagger(x) [i\Gamma^\mu (\partial_\mu - i a_\mu) - M S^z] \psi(x) \\ &= \int dx \psi^\dagger(x) [i\Gamma^\mu \partial_\mu - M S^z] \psi(x) \\ &\quad + \int dx \psi^\dagger(x) \Gamma^\mu a_\mu \psi(x) = L_0 + L_{int}. \end{aligned} \quad (4.5)$$

Gauge potentials are defined by $a_\mu = iU^\dagger \partial_\mu U = S^x \partial_\mu \theta$. In keeping with the Γ -matrix notation of the Dirac Hamiltonian we employ a similar notation for $\Gamma^0 = \mathbb{I}$, $\Gamma^1 = S^x$.

It is our task to compute the expectation value of the current $j^\mu = \psi^\dagger \Gamma^\mu \psi$

$$\begin{aligned} \langle j^\mu(x) \rangle &= -i \text{tr} (\Gamma^\mu G_0(0)) \\ &\quad - i \int d^2 z \text{tr} (\Gamma^\mu G_0(x-z) \Gamma^\nu a_\nu G_0(z-x)), \end{aligned} \quad (4.6)$$

where the free propagator G_0 is

$$\begin{aligned} G_0(x-y) &\equiv \text{Tr} \left(\frac{i}{-i\partial_t - H_0} \right) \\ &= \int \frac{dw dk_x}{(2\pi)^2} \frac{i}{w(w^2 - k_x^2 - M^2)} \begin{pmatrix} w^2 - \frac{k_x^2}{2} + Mw & \frac{k_x w}{\sqrt{2}} + \frac{k_x M}{\sqrt{2}} & \frac{k_x^2}{2} \\ \frac{k_x w}{\sqrt{2}} + \frac{k_x M}{\sqrt{2}} & w^2 - M^2 & \frac{k_x w}{\sqrt{2}} - \frac{k_x M}{\sqrt{2}} \\ \frac{k_x^2}{2} & \frac{k_x w}{\sqrt{2}} - \frac{k_x M}{\sqrt{2}} & w^2 - \frac{k_x^2}{2} - Mw \end{pmatrix} e^{ik \cdot (x-y)}, \end{aligned} \quad (4.7)$$

where we use the notation $x_\mu = (t, -x)$, $k_\mu = (w, -k_x)$ and $k \cdot x = k^\mu x_\mu = wt - k_x x$. The first term of (4.6) reads

$$\begin{aligned} -i \text{tr} (\Gamma^1 G_0(0)) &= \int \frac{dw dk_x}{(2\pi)^2} \left(\frac{2w}{w^2 - k_x^2 - M^2} \right) = 0, \\ -i \text{tr} (G_0(0)) &= \int \frac{dw dk_x}{(2\pi)^2} \left(\frac{1}{w} + \frac{2w}{w^2 - k_x^2 - M^2} \right) = \int \frac{dw dk_x}{(2\pi)^2} \left(\frac{1}{w} \right). \end{aligned} \quad (4.8)$$

It seems that this term gives infra-red (IR) divergence ($w \rightarrow 0$). The divergence comes from the $E = 0$ flat band. However, since we set the Fermi energy slightly below the flat band ($E_F = 0^-$), the $E = 0$ pole is not included in the contour integral Fig. 1. Thus we have

$$\langle j^\mu(q) \rangle = \Pi^{\mu\nu}(q) a_\nu(q) = -i \int \frac{dw dk_x}{(2\pi)^2} \text{tr} \left[\left(\frac{i}{-i\partial_t - H_0} \right)_{k-q} \Gamma^\mu \left(\frac{i}{-i\partial_t - H_0} \right)_k \Gamma^\nu a_\nu(q) \right]. \quad (4.9)$$

In the large- M limit, which is equivalent to the small q limit, the current average becomes

$$\langle j^\mu(q) \rangle \simeq -i \int \frac{dw dk_x}{(2\pi)^2} \text{tr} \left[\frac{i}{w - k_x S^x - M S^z} \Gamma^\mu \frac{i}{w - k_x S^x - M S^z} \Gamma^\nu \Gamma^1 \right] \partial_\nu \theta(q). \quad (4.10)$$

Using (4.7) we compute the traces

$$\begin{aligned} \text{tr}[G_0 \Gamma^1 G_0 \Gamma^1 \Gamma^1] &= \frac{2k_x(M^2 - 2w^2)}{w(k_x^2 + M^2 - w^2)^2}, \\ \text{tr}[G_0 \Gamma^1 G_0 \Gamma^0 \Gamma^1] &= -\frac{2(k_x^2 - M^2 + w^2)}{(k_x^2 + M^2 - w^2)^2}, \\ \text{tr}[G_0 \Gamma^0 G_0 \Gamma^1 \Gamma^1] &= -\frac{M^2(k_x^2 + M^2 - w^2) + 2w^2(k_x^2 + w^2)}{w^2(k_x^2 + M^2 - w^2)^2}, \\ \text{tr}[G_0 \Gamma^0 G_0 \Gamma^1] &= -\frac{4k_x w}{(k_x^2 + M^2 - w^2)^2}. \end{aligned} \quad (4.11)$$

The first and fourth terms in (4.11) are odd functions in k_x thus their contributions vanish after the k_x -integration. Integrating (4.10) over w and k_x we have

$$\begin{aligned} \langle j^0 \rangle &= -i \int \frac{dk_x dw}{(2\pi)^2} \text{tr}[G_0 \Gamma^0 G_0 \Gamma^1 \Gamma^1] \partial_1 \theta \\ &= i \int \frac{dk_x dw}{(2\pi)^2} \frac{M^2(k_x^2 + M^2 - w^2) + 2w^2(k_x^2 + w^2)}{w^2(k_x^2 + M^2 - w^2)^2} \partial_1 \theta \\ &= -\frac{1}{2\pi} \int dk_x \frac{M^2}{(k_x^2 + M^2)^{3/2}} \partial_1 \theta \\ &= -\frac{1}{\pi} \partial_1 \theta, \end{aligned} \quad (4.12)$$

and

$$\begin{aligned} \langle j^1 \rangle &= -i \int \frac{dk_x dw}{(2\pi)^2} \text{tr}[G_0 \Gamma^1 G_0 \Gamma^0 \Gamma^1] \partial_0 \theta \\ &= i \int \frac{dk_x dw}{(2\pi)^2} \frac{2(k_x^2 - M^2 + w^2)}{(k_x^2 + M^2 - w^2)^2} \partial_0 \theta \\ &= \frac{1}{2\pi} \int dk_x \frac{M^2}{(k_x^2 + M^2)^{3/2}} \partial_0 \theta \\ &= \frac{1}{\pi} \partial_0 \theta, \end{aligned} \quad (4.13)$$

where the integration contour for the w -integration is taken over the closed path not enclosing the positive and zero frequency poles as shown in Fig. 1.

Combining (4.12) and (4.13) we obtain

$$\langle j^\mu \rangle = -\frac{1}{\pi} \epsilon^{\mu\nu} \partial_\nu \theta = -\frac{1}{\pi} \epsilon^{\mu\nu} \partial_\nu \tan^{-1} \left(\frac{\phi_1}{\phi_2} \right). \quad (4.14)$$

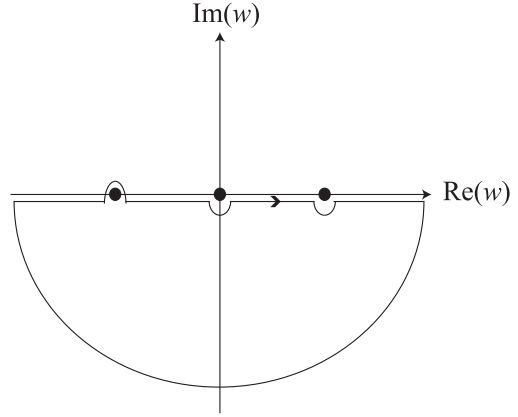


FIG. 1: Integration contour of w .

Integrating the j^0 over x we easily compute the charge

$$Q = -\frac{1}{\pi} \Delta \left(\tan^{-1} \left(\frac{\phi_1}{\phi_2} \right) \right). \quad (4.15)$$

In the case where $\phi_2(x)$ behaves as a solitonic background, i.e. $\phi_2(x) \rightarrow \pm \delta t_0$ as $x \rightarrow \pm \infty$ and $\phi_1(x) = m_0$, we have

$$Q = -\frac{2}{\pi} \tan^{-1} \left(\frac{\delta t_0}{m_0} \right). \quad (4.16)$$

This result supports our previous quantum mechanical charge computation.

¹ R. Jackiw and G. W. Semenoff, Phys. Rev. Lett. **50**, 439 (1983); R. MacKenzie and Frank Wilczek, Phys. Rev. D **30**, 2194 (1984)

² J. Goldstone and F. Wilczek, Phys. Rev. Lett. **47**, 986 (1981).